E1-2005-104

N. Giokaris[1], A. Antonaki[1], I. Fedorko[1],
V. Giakoumopoulou[1], A. Manousakis-Katsikakis[1],
A. Staveris-Polykalas[1], C. Vellidis[1], J. Budagov,
G. Chlachidze, V. Glagolev, A. Sissakian

PROBING THE TOP-QUARK MASS IN THE DILEPTON AND LEPTON+JETS CHANNELS USING ONLY LEPTON INFORMATION

Submitted to «Particles and Nuclei, Letters»

[1] Department of Physics, Division of Nuclear and Particle Physics, University of Athens, Greece

Джиокарис Н. и др. E1-2005-104
Определение массы топ-кварка в каналах dilepton
и lepton+jets на основе только измеренных данных о лептонах

Предложен новый метод измерения массы топ-кварка — метод, использующий только измеренные величины поперечных импульсов электронов и мюонов, рожденных в процессе $t\bar{t} \to$ dilepton и $t\bar{t} \to$ lepton+jets. Показано, что эти переменные «чувствительны» к величине массы топ-кварка. Этот импульс, будучи достаточно точно измеренным, позволяет получить массу топ-кварка с незначительной систематической погрешностью и, при достаточно высокой светимости, с небольшой статистической погрешностью.

Работа выполнена в Лаборатории ядерных проблем им. В. П. Джелепова ОИЯИ.

Препринт Объединенного института ядерных исследований. Дубна, 2005

Giokaris N. et al. E1-2005-104
Probing the Top-Quark Mass in the Dilepton and Lepton+Jets
Channels Using Only Lepton Information

A new method of extracting the top-quark mass is proposed. It uses only information on the transverse momentum of electrons and muons produced in the $t\bar{t} \to$ dilepton and $t\bar{t} \to$ lepton+jets decay channels. It is shown that this variable, among others, is sensitive to the top-quark mass. As it is very accurately measured, it can provide the top-quark mass with a very small systematic error and, at high enough integrated luminosity, with a very small total error.

The investigation has been performed at the Dzhelepov Laboratory of Nuclear Problems, JINR.

Preprint of the Joint Institute for Nuclear Research. Dubna, 2005

1. INTRODUCTION

The top quark was discovered by the CDF and D0 collaborations at the Fermilab Tevatron in 1995 [1]. Subsequent publications gave more details on its kinematic properties [2, 3, 4, 5, 6, 7, 8]. Presently an intensive effort is under way, in both Tevatron experiments, to measure its mass with the highest possible accuracy [9]. The desired accuracy is necessary in many constraints that we can put on the Standard Model (SM), for example, on the mass of the Higgs boson [1].

In addition, much work has also been done (at the level of simulations) by the ATLAS [10] and CMS [11] collaborations in the perspective of the future experiments using the LHC at CERN.

A brief summary on the latest measurements of the top-quark mass and on the methods pursued for this purpose is given here. Several factors contribute to the systematic error of the measured top-quark mass. However, the main contribution comes from the uncertainty in the jet energy scale [2, 9].

The motivation for the proposed technique of measuring the top-quark mass will be presented in Sec. 2. The sensitivity of the lepton transverse kinematics to the top-quark mass at both the Tevatron and LHC energies will be examined in Sec. 3. Then, in Sec. 4, the expected statistical and systematic errors will be discussed. In Appendix A, the derived sensitivity of the lepton momentum to the top-quark mass will be investigated. Finally, in Appendix B, certain computational requirements for the achievement of a highly accurate result will be briefly discussed.

2. MOTIVATION FOR THE PROPOSED TECHNIQUE

Presently the statistical and the systematic errors of the top-quark mass are nearly equal and at the level of about ± 3 GeV, using data from either the CDF or D0 experiment [9]. As the integrated luminosity increases, the statistical error will decrease and the systematic error will dominate. This will be particularly true for the LHC experiments, where a huge number of top candidate events will be registered, even by the end of the first year of operation [10, 11]. However, as mentioned above, the main source of the systematic error still will be the uncertainty in the jet energy scale.

A way to bypass this problem is to use physical quantities other than the jet energies, such that they are sensitive to the top-quark mass and they can be measured very precisely. It is proposed here to use the transverse momentum of

the leptons in the $t\overline{t} \rightarrow$ dilepton and $t\overline{t} \rightarrow$ lepton+jets decay modes, where the leptons are electrons ($+$ or $-$) and/or muons ($+$ or $-$).

3. DESCRIPTION OF THE PROPOSED TECHNIQUE

At the Tevatron ($p\overline{p}$ collisions at $\sqrt{s} = 1.96$ TeV) top quarks are produced mainly in pairs through $q\overline{q}$ annihilation into a gluon and subsequent split into a $t\overline{t}$ pair as shown in Fig. 1.

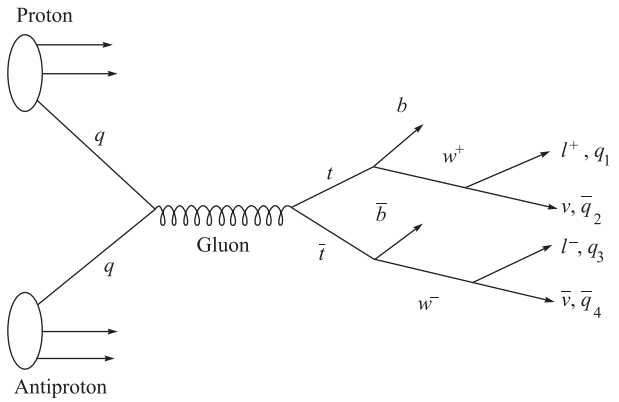

Fig. 1. Top-quark production through $q\overline{q}$ annihilation

According to the SM, each top (t) quark decays into a W boson and a bottom (b) quark (see Fig. 1). For this study, $t\overline{t}$ pairs have been generated (for Tevatron conditions) using the Herwig Monte Carlo program [12]. Events where both W bosons decay into a lepton and a neutrino (dilepton mode), have been selected. Further requirements are that both of the leptons are electrons and/or muons and that they have opposite electric charge. Two additional cuts on the lepton transverse momenta, $P_T > 20$ GeV/c, and on their pseudorapidities, $|\eta| < 1.1$, are imposed. The spectrum of the lepton transverse momentum (two entries per $t\overline{t}$ event) for a top-quark mass of 180 GeV/c^2 is shown in Fig. 2. Similar spectra have been obtained for a top-quark mass of 130, 150, 160, 170, 190, 200, 210, and 230 GeV/c^2. The mean value $\langle P_T \rangle$ of the lepton's P_T and its standard deviation vs. the top-quark mass are listed in Table 1. The mean value of the lepton's P_T is shown in Fig. 3 as a function of the top-quark mass.

It is seen that the lepton's $\langle P_T \rangle$ is sensitive to the top-quark mass $M_{\rm top}$. A fit of a straight line of the form

$$\langle P_T \rangle = \kappa + \lambda M_{\rm top} \tag{1}$$

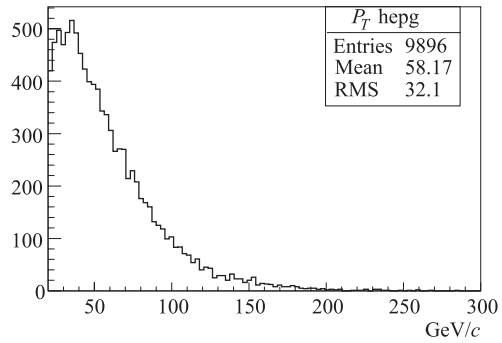

Fig. 2. Distribution of the lepton's P_T at generation level for $p\overline{p}$ collisions at $\sqrt{s} = 1.96$ TeV for $M_{\rm top} = 180$ GeV/c^2

Table 1. The lepton's $\langle P_T \rangle$ and its standard deviation vs. the top-quark mass at generation level for $p\overline{p}$ collisions at $\sqrt{s} = 1.96$ TeV

Top-quark mass, GeV/c^2	Lepton $\langle P_T \rangle$, GeV/c	P_T standard deviation, GeV/c
130	50.59	26.15
150	53.33	28.43
160	55.08	30.39
170	56.78	31.55
180	58.17	32.10
190	58.91	31.73
200	60.83	34.21
210	62.72	34.73
230	67.11	37.64

gives a $\chi^2/\text{n.d.f.}$ of 2.8 and a slope of $\lambda = 0.16$. Similar fits have been done also for the lepton's total momentum, the leading lepton's total and transverse momenta, the sum of the P_T's of the two leptons, the sum of the total momenta of the two leptons and the invariant mass of the two leptons. The slopes of the straight line fits to the mean values of all these variables, as functions of the top-quark mass, are given in Table 2.

As expected, the variable most sensitive to the top-quark mass is the sum of the total momenta of the two leptons, having a slope of 0.35. However, we would like to use a variable that is invariant under Lorentz transformations along the colliding beams and that is also the same for both the $t\overline{t} \rightarrow$ dilepton and $t\overline{t} \rightarrow$ lepton+jets decay modes. The P_T of each lepton is such a variable.

The next step was to study the effect of the detector resolution and of the selection cuts on the mean value of the lepton's P_T, on its standard deviation

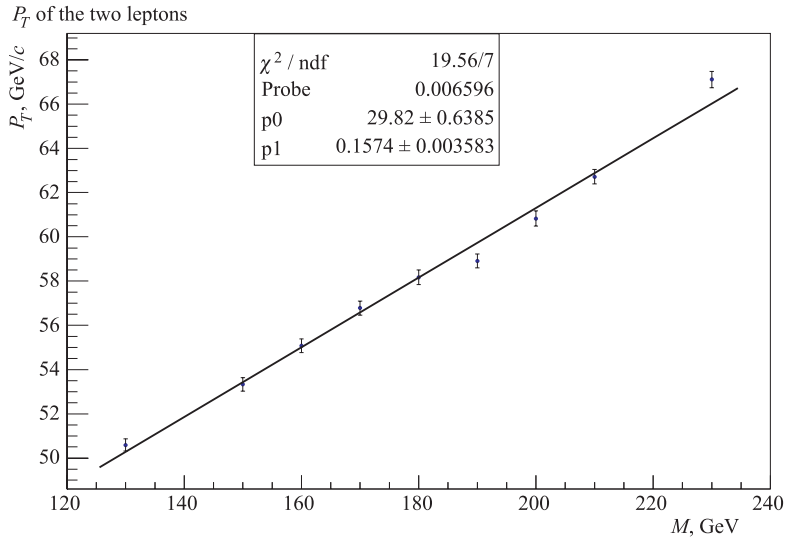

Fig. 3. The lepton's $\langle P_T \rangle$ vs. the top-quark mass at generation level for $p\overline{p}$ collisions at $\sqrt{s} = 1.96$ TeV

Table 2. Slopes of various lepton kinematic variables vs. the top-quark mass at generation level for $p\overline{p}$ collisions at $\sqrt{s} = 1.96$ TeV

Variable	Slope
$\langle P_T \rangle$	0.1574 ± 0.0036
$\langle P \rangle$	0.1739 ± 0.0042
Leading $\langle P_T \rangle$	0.2278 ± 0.0054
Leading $\langle P \rangle$	0.2523 ± 0.0064
Sum of $\langle P_T \rangle$'s	0.3160 ± 0.0080
Sum of $\langle P \rangle$'s	0.3523 ± 0.0092
Invariant mass	0.2211 ± 0.0095

and on the slope of the straight line of $\langle P_T \rangle$ vs. the top-quark mass. For this purpose, a full simulation for a CDF Run II type of a detector [13] has been performed using the $t\overline{t} \rightarrow$ dilepton events. Then, all of the CDF type cuts were applied. Table 3 lists the mean value of the P_T of the two leptons and its standard deviation vs. the top-quark mass. Table 4 gives the slopes of the straight line fits to the mean values of the same variables that are listed in Table 2. It is seen that resolution and selection cuts have a very small combined effect on the width of the P_T spectrum and, therefore, on the ultimate statistical error of the top-quark mass extracted using this method at a given luminosity. The mean value of P_T is shown in Fig. 4 as a function of the top-quark mass.

Table 3. The lepton's $\langle P_T \rangle$ and its standard deviation vs. the top-quark mass after simulation for $p\overline{p}$ collisions at $\sqrt{s} = 1.96$ TeV

Top-quark mass, GeV/c^2	Lepton $\langle P_T \rangle$, GeV/c	P_T standard deviation, GeV/c
130	54.43	30.00
150	57.24	31.94
160	59.54	33.55
170	60.99	34.12
180	63.43	35.47
190	62.85	34.82
200	65.86	37.86
210	66.54	37.58
230	70.17	38.79

Table 4. Slopes of various lepton kinematic variables vs. the top-quark mass after simulation for $p\overline{p}$ collisions at $\sqrt{s} = 1.96$ TeV

Variable	Slope
$\langle P_T \rangle$	0.1546 ± 0.0106
$\langle P \rangle$	0.1766 ± 0.0122
Leading $\langle P_T \rangle$	0.2172 ± 0.0157
Leading $\langle P \rangle$	0.2309 ± 0.0182
Sum of $\langle P_T \rangle$'s	0.3091 ± 0.0237
Sum of $\langle P \rangle$'s	0.3317 ± 0.0273

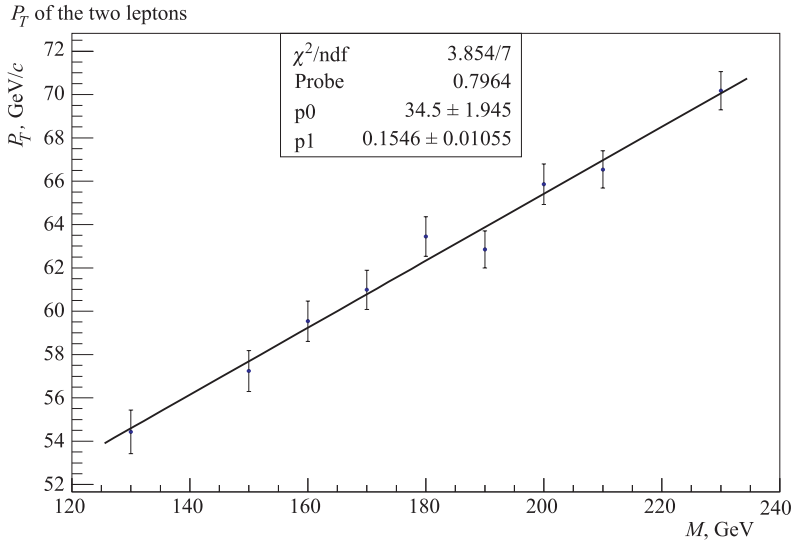

Fig. 4. The lepton's $\langle P_T \rangle$ vs. the top-quark mass after simulation for $p\overline{p}$ collisions at $\sqrt{s} = 1.96$ TeV

Next, the validity of the technique at LHC conditions (pp collisions at $\sqrt{s} = 14$ TeV [10]) has been examined. At the LHC the top-quark is produced in pairs through gluon–gluon fusion into a gluon and its subsequent split into $t\bar{t}$ as shown in Fig. 5. The Pythia Monte Carlo program [14] has been used to generate this kind of events. Again, $t\bar{t} \rightarrow$ dilepton events have been selected, the two leptons being electrons and/or muons. In Table 5, the $\langle P_T \rangle$ of the leptons and its standard deviation are listed as functions of the top-quark mass. Table 6 gives the slopes of the straight line fits to the mean values of the same variables that are listed in Table 2. Comparing Tables 2 and 6 we see that these slopes are generally higher for the LHC conditions than for the Tevatron conditions.

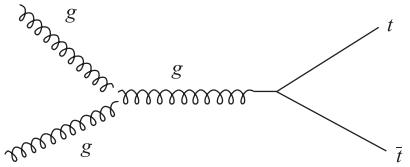

Fig. 5. Main Feynman diagram for top-quark production at LHC

Table 5. The lepton's $\langle P_T \rangle$ and its standard deviation vs. the top-quark mass at generation level for pp collisions at $\sqrt{s} = 14$ TeV

Top-quark mass, GeV/c^2	Lepton $\langle P_T \rangle$, GeV/c	P_T standard deviation, GeV/c
130	54.99	33.13
140	55.50	33.47
150	57.37	35.75
160	59.37	37.10
170	61.69	38.97
180	63.89	40.83
190	66.28	43.91
200	67.63	44.52
210	69.81	45.11
220	72.67	47.32
230	75.65	51.03

Again, only two requirements were imposed: that the P_T's of both leptons are larger than 20 GeV/c and that their pseudorapidities are absolutely less than 1.1. The relation of $\langle P_T \rangle$ with the top-quark mass is again linear as shown in Fig. 6. The slope of the corresponding straight line is 0.21 with a $\chi^2/\mathrm{n.d.f.}$ of 3, similar to the values obtained at the Tevatron energy.

Table 6. Slopes of various lepton kinematic variables vs. the top-quark mass at generation level for pp collisions at $\sqrt{s} = 14$ TeV

Variable	Slope
$\langle P_T \rangle$	0.2068 ± 0.0039
$\langle P \rangle$	0.2420 ± 0.0048
Leading $\langle P_T \rangle$	0.3020 ± 0.0061
Leading $\langle P \rangle$	0.3526 ± 0.0075
Sum of $\langle P_T \rangle$'s	0.3981 ± 0.0083
Sum of $\langle P \rangle$'s	0.4520 ± 0.0097

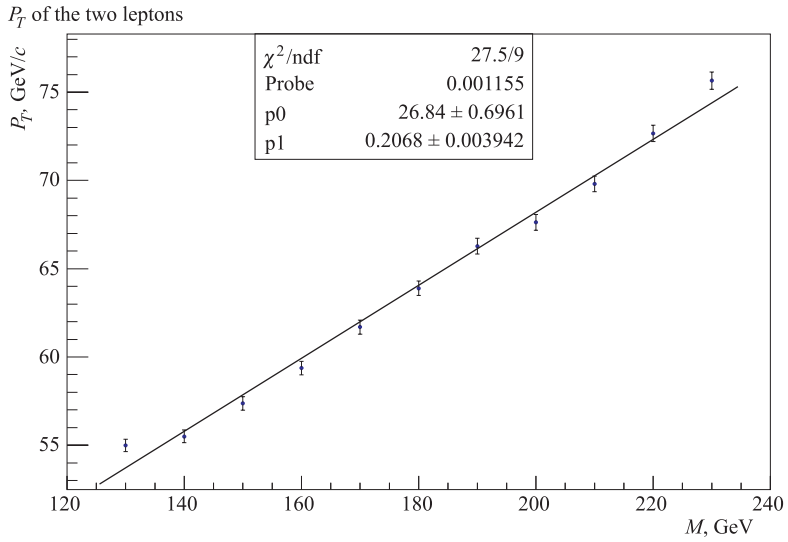

Fig. 6. The lepton's $\langle P_T \rangle$ vs. the top-quark mass at generation level for pp collisions at $\sqrt{s} = 14$ TeV

The above results show that the top-quark mass can be extracted from the P_T distribution of $t\bar{t} \to$ dilepton events by using the solution of Eq. (1) for $M_{\rm top}$ in terms of $\langle P_T \rangle$:

$$M_{\rm top} = \frac{\langle P_T \rangle - \kappa}{\lambda} \tag{2}$$

with the parameters κ and λ derived from the fit appropriate for the Tevatron or for the LHC conditions.

4. ESTIMATION OF ERRORS

The expected statistical error in the top-quark mass as extracted from the P_T spectrum of the two leptons in the $t\overline{t} \rightarrow$ dilepton mode is a function of the expected Tevatron integrated luminosity $\mathcal{L}$ and is given in Table 7 [15]. The error $(\delta M_{\rm top})_{\rm stat}$ has been estimated using the formula

$$(\delta M_{\rm top})_{\rm stat} = \frac{(\delta \langle P_T \rangle)_{\rm stat}}{\lambda} = \frac{1}{\lambda} \times \frac{P_T^{\rm rms}}{\sqrt{N}} \tag{3}$$

derived from Eq. (2). $P_T^{\rm rms}$ is the standard deviation of the P_T distribution (35.47 GeV/c from the simulation results listed in Table 3); N is twice the number of the reconstructed $t\overline{t} \rightarrow$ dilepton events (two leptons per event); and $\lambda = 0.1546$ is the slope of the straight line of the lepton's transverse momentum vs. the top-quark mass (see Table 4). The number N has been estimated from the relation

$$N = 2N_{t\overline{t}} = 2B_{e\mu}\,\varepsilon\,\sigma\left(p\overline{p} \rightarrow t\overline{t}\right)\mathcal{L}. \tag{4}$$

A $t\overline{t}$-production cross section $\sigma\left(p\overline{p} \rightarrow t\overline{t}\right)$ of 7 pb [16], $B_{e\mu}\,\varepsilon = 0.75\%$ branching ratio $\times$ efficiency product of $t\overline{t} \rightarrow e^+e^-$, $e^+\mu^-$, μ^+e^- and $\mu^+\mu^-$ pairs, and a top-quark mass of $M_{\rm top} = 180$ GeV/c^2 have been assumed.

Table 7. The statistical error in the top-quark mass from the P_T spectrum of the two leptons in the $t\overline{t} \rightarrow$ dilepton events as a function of the expected Tevatron integrated luminosity

Integrated, luminosity, pb^{-1}	Expected by	Expected number of dilepton events	$(\delta M_{\rm top})_{\rm stat}$	
			GeV/c^2	%
193	Feb. 2003	10	51	28
400	Sep. 2004	21	35	20
1200	Dec. 2005	63	20	11
3000	Dec. 2006	158	13	7
8000	Dec. 2008	420	8	4

A further reduction of the statistical error by a factor of about 2 can be achieved if the similar measurement of the top-quark mass from the P_T spectrum of the lepton (e or μ) in the $t\overline{t} \rightarrow$ lepton+jets decay mode is combined with the one from the dilepton events.

The above exercise has also been done for the LHC/ATLAS conditions [10]; i. e., pp collisions at $\sqrt{s} = 14$ TeV, a $t\overline{t}$-production cross section of 800 pb for $M_{\rm top} = 180$ GeV/c^2, an ATLAS type $t\overline{t} \rightarrow$ dilepton branching ratio $\times$ efficiency product equal to 1%, a standard deviation of the P_T distribution equal to 40.83

GeV/c (see Table 5), and a slope of P_T vs. $M_{\rm top}$ equal to 0.2068 (see Table 6). The corresponding errors in the top-quark mass are listed in Table 8. It is seen that by the end of the first year of LHC operation a statistical error in $M_{\rm top}$ of down to about 1.5 GeV/c^2 can be achieved.

Table 8. The statistical error in the top-quark mass from the P_T spectrum of the two leptons in the $t\bar{t} \rightarrow$ dilepton events as a function of the expected LHC integrated luminosity

Integrated luminosity, pb^{-1}	Expected by	Expected number of dilepton events	$(\delta M_{\rm top})_{\rm stat}$	
			GeV/c^2	%
1000	End of the 1st year of operation	8000	1.6	0.8
10,000	End of the 2nd year of operation	80 000	0.5	0.3

It should be noted that at LHC a statistically more accurate $M_{\rm top}$ value can be obtained by using the sum of the P_T's of the two leptons in each $t\bar{t} \rightarrow$ dilepton event (see Table 6).

The systematic error in the top-quark mass derived from Eq. (2) is given by

$$(\delta M_{\rm top})_{\rm syst} = \frac{1}{\lambda} \times \sqrt{(\delta \langle P_T \rangle)^2_{\rm syst} + (\delta\kappa)^2 + M^2_{\rm top}\,(\delta\lambda)^2}, \qquad (5)$$

i. e., it is determined by the systematic error in the estimated mean of the lepton's P_T distribution and by the errors in the parameters of the linear fit: the constant term κ and the slope λ. A number of sources contribute to the individual errors of Eq. (5):

1. The uncertainty in the fit parameters due to the finite Monte Carlo statistics and the omission of nonlinear terms. This is provided by the least squares algorithm.
2. The uncertainty in the measurement of the lepton's P_T.
3. The uncertainty in the measurement of the transverse energy E_T of the jets, implying also an uncertainty in the missing transverse energy $\not\!\!E_T$.
4. The theoretical uncertainties of the Monte Carlo event generator.
5. The uncertainty in the knowledge of the background.

In what follows, we briefly discuss each of the last four sources of error for the Tevatron/CDF conditions and for the $t\bar{t} \rightarrow$ dilepton channel.

The electron E_T and the muon P_T scales are presently known at CDF down to 30 MeV and 50 MeV/c, respectively, from the study of $Z \rightarrow e^+e^-$ and $Z \rightarrow \mu^+\mu$ events [13].

There are two types of theoretical uncertainties in the Monte Carlo event generator: one is related with the parton distribution functions (PDF) of the proton; and the other, with the modeling of soft gluon radiation from the initial-state quarks (ISR) and/or from the final-state top quarks (FSR). Also important is the final-state electromagnetic radiation (bremsstrahlung) from the leptons. Although this effect is well under control in the framework of QED, it must be taken into account as it alters the lepton kinematics. The error in the fit parameters κ and λ due to the uncertainty in the choice of PDF's has been estimated by trying two generators using different PDF's: Herwig [12] and Pythia [14]. The estimated mean values of the lepton kinematic variables at $M_{\rm top} = 180$ GeV/c^2 are listed in Table 9. It is seen that the results from the two generators agree perfectly well within the standard errors of the Monte Carlo statistics. It follows that the errors in κ and λ due to this source of uncertainty are consistent with zero. The errors due to the uncertainty in the gluon radiation are currently under study.

Table 9. The mean values of various lepton kinematic variables estimated using two different Monte Carlo generators for $p\overline{p}$ collisions at $\sqrt{s} = 1.96$ TeV and for top-quark mass $M_{\rm top} = 180$ GeV/c^2

Variable	Pythia	Herwig
$\langle P_T \rangle$	58.00 ± 0.32	58.17 ± 0.32
$\langle P \rangle$	67.48 ± 0.38	67.63 ± 0.38
Leading $\langle P_T \rangle$	72.90 ± 0.50	73.52 ± 0.50
Leading $\langle P \rangle$	85.59 ± 0.60	85.98 ± 0.59
Sum of $\langle P_T \rangle$'s	116.2 ± 0.7	116.6 ± 0.7
Sum of $\langle P \rangle$'s	135.4 ± 0.8	135.6 ± 0.8

The uncertainty in the jet energy scale has an indirect effect on $\langle P_T \rangle$, namely because of the cuts on the E_T of jets and on the E_T in the event. It has been estimated by the difference in the lepton's $\langle P_T \rangle$ for the nominal jet energy scale and for the case where the jet energies have been varied by $\pm 10\%$ on a sample of Herwig Monte Carlo events assuming $M_{\rm top} = 180$ GeV/c^2. The resulting lepton's $\langle P \rangle$ and $\langle P_T \rangle$ are listed in Table 10 and they agree within the standard errors of the Monte Carlo statistics for all three scales chosen for the jet energies. Hence the error in $\langle P_T \rangle$ due to the uncertainty in the jet energy scale is again consistent with zero.

A full study of the systematic uncertainties associated with the method presented here is currently underway and will be discussed in detail in a forthcoming paper.

Table 10. The effect on the lepton's $\langle P_T \rangle$ and $\langle P \rangle$ of variations in the jet energy scale and in E_T after simulation for $p\overline{p}$ collisions at $\sqrt{s} = 1.96$ TeV

E_T(jet), E_T shift, %	$\langle P_T \rangle$, GeV/c	$\langle P \rangle$, GeV/c
No shift	63.45 ± 0.91	72.35 ± 1.05
$+10\%$ E_T(jet), -10% $\not\!\!E_T$	64.08 ± 0.96	72.43 ± 1.09
-10% E_T(jet), $+10\%$ $\not\!\!E_T$	63.41 ± 0.90	71.87 ± 1.03

APPENDIX A: TEST OF THE MONTE CARLO RESULTS

We can understand the small and constant slopes of the lepton kinematics with respect to the top-quark mass by looking more closely to the kinematics of $t\overline{t}$-pair production. The cross section for $t\overline{t}$-pair production in $p\overline{p}$ collisions can be written in the form [17]

$$\sigma\left(p\overline{p} \to t\overline{t}\right) = \sum_{i,j} \int dx_i F_i\left(x_i \mu^2\right) \int dx_j F_j\left(x_j\,, \mu^2\right) \hat{\sigma}_{ij}\left(\hat{s}, \mu^2, M_{\rm top}\right), \quad (6)$$

F_i and F_j are the number densities of light partons (quarks, antiquarks, and gluons) evaluated at a scale μ in the proton and antiproton; x_i and x_j are the momentum fractions of the incoming partons [i. e., the parton $i(j)$ has momentum $x_i P(-x_j P)$, where P is the magnitude of the proton momentum in the center-of-mass frame (which in colliding beam experiments coincides with the laboratory frame)]; $\hat{\sigma}_{ij}$ is the point cross section for $i + j \to t\overline{t}$; and $\hat{s} = 4x_i x_j P^2 = 4x_i x_j s$ is the square of the center-of-mass energy of the parton–parton collision.

We are primarily interested in the cross section for the $q\overline{q} \to t\overline{t}$ subprocess which, for large $M_{\rm top}$, dominates at the Tevatron energy. This is given in the lowest order by [18]

$$\hat{\sigma}\left(q\overline{q} \to t\overline{t}\right) = \frac{8\pi\alpha_s}{27\hat{s}}\left(1 + \frac{2M_{\rm top}^2}{\hat{s}}\right)\sqrt{1 - \frac{\left(2M_{\rm top}\right)^2}{\hat{s}}}. \quad (7)$$

As a function of $\hat{s}$, $\hat{\sigma}$ rises from threshold ($\hat{s} = 4M_{\rm top}^2$), reaches a maximum at

$$\hat{s} = \frac{20}{\sqrt{21} - 1} M_{\rm top}^2 \approx 5.6 M_{\rm top}^2$$

and then falls off asymptotically as $1/\hat{s}$. When convoluted with the $q\overline{q}$ density functions, according to Eq. (6), the maximum of the $q\overline{q} \to t\overline{t}$ cross section is shifted down to $\hat{s} \approx 4.5 M_{\rm top}^2$. Therefore, the most probable energy for a top-quark produced by $q\overline{q}$ annihilation is $E_{\rm top} \approx \sqrt{4.5} M_{\rm top}/2 \approx 1.06 M_{\rm top}$ and the corresponding most probable momentum is $P_{\rm top} \approx 0.35 M_{\rm top}$. For example, for a top quark of mass $M_{\rm top} = 175$ GeV/c^2 the most probable momentum is $P_{\rm top} = 62$ GeV/c and the most probable kinetic energy is $T_{\rm top} = E_{\rm top} - M_{\rm top} = 10.6$ GeV.

These conditions are not far from the $t\bar{t}$-production threshold, i. e., from the point where each top quark is produced at rest. At this point the momentum of each lepton produced by the $t\bar{t}$-pair decay in the laboratory frame is

$$P_{\rm lepton} = \frac{1}{4M_{\rm top}} \left\{ M_{\rm top}^2 + M_W^2 - M_b^2 + \right.$$
$$\left. + \sqrt{\left[M_{\rm top}^2 - (M_W + M_b)^2\right]\left[M_{\rm top}^2 - (M_W - M_b)^2\right]}\cos\theta_{\rm lepton} \right\}, \quad (8)$$

where $\theta_{\rm lepton}$ is the lepton emission angle in the rest frame of the W boson, M_W and M_b are the masses of the W boson and of the b quark, respectively, and the mass of the lepton (electron or muon) has been omitted. The average lepton momentum is then

$$\langle P_{\rm lepton}\rangle = \frac{M_{\rm top}^2 + M_W^2 - M_b^2}{4M_{\rm top}}, \quad (9)$$

and its slope with respect to the top-quark mass is

$$\frac{d\langle P_{\rm lepton}\rangle}{dM_{\rm top}} = \frac{M_{\rm top}^2 - M_W^2 + M_b^2}{(2M_{\rm top})^2}. \quad (10)$$

It is immediately seen that, for $M_{\rm top}$ much larger than M_W, the lepton momentum averages near $M_{\rm top}$/4, and its slope with respect to the top-quark mass averages near 1/4. Table 11 lists the values of the average lepton momentum and

Table 11. The expected $\langle P_{\rm lepton}\rangle$ and $d\langle P_{\rm lepton}\rangle/dM_{\rm top}$ at the $t\bar{t}$-production threshold

$M_{\rm top}$, GeV/c^2	$\langle P_{\rm lepton}\rangle$, GeV/$c$	$d\langle P_{\rm lepton}\rangle/dM_{\rm top}$
130	44.89	0.1547
140	46.51	0.1678
150	48.24	0.1784
160	50.07	0.1871
170	51.98	0.1943
180	53.95	0.2003
190	55.98	0.2054
200	58.05	0.2097
210	60.17	0.2135
220	62.32	0.2167
230	64.50	0.2195

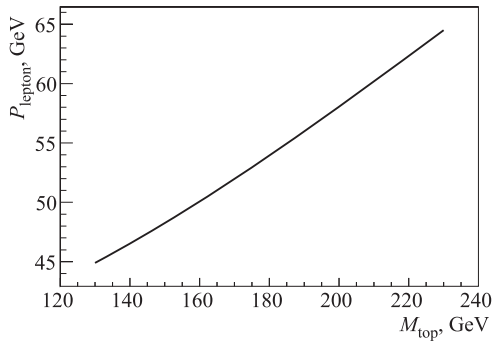

Fig. 7. The expected $\langle P_{\text{lepton}} \rangle$ vs. the top-quark mass at the $t\bar{t}$-production threshold

of its slope as functions of the top-quark mass, calculated according to Eqs. (9) and (10), respectively, for $M_W = 80.4$ GeV/c^2 and $M_b = 4.5$ GeV/c^2 [19]. The average lepton momentum is plotted against the top-quark mass in Fig. 7 and shows that the change of its slope with the top-quark mass is too small to be detected by the Monte Carlo fit with the present accuracy. The expected slope at threshold averages 0.195 over the scanned mass range. This result is fairly close to both the slope 0.174 ± 0.004 of $\langle P \rangle$ given in Table 2 for the Tevatron conditions and the slope 0.242 ± 0.005 of $\langle P \rangle$ given in Table 6 for the LHC conditions. For the LHC conditions, the slope is higher because of gluon radiation from the top quarks: heavier top quarks radiate softer gluons, transferring thus more kinetic energy to their decay products. For the Tevatron conditions, gluon radiation is suppressed due to lower total energy. In this case the slope is lower than the expected threshold value because of the finite momentum of the top-quarks that smears out the sensitivity of the lepton kinematics to the top-quark mass.

APPENDIX B: OPTIMIZATION OF THE FIT

We briefly examine the methodology for improving the fit of the functional relationship between $\langle P_T \rangle$ and M_{top} to the Monte Carlo data in order to meet the desired accuracy. Let P_i be the values of $\langle P_T \rangle$ corresponding to the $i = 1, \ldots, n$ trial values M_i of the top-quark mass M_{top}. The errors associated with the mean values P_i are estimated by $P_i/\sqrt{N_i}$, where N_i is the number of $t\bar{t} \to$ dilepton Monte Carlo events passing all of the selection cuts after simulation. Defining

$$S_{\kappa\kappa} \equiv \sum_{i=1}^{n} \frac{N_i}{P_i^2}, \qquad S_{\kappa\lambda} \equiv \sum_{i=1}^{n} \frac{N_i M_i}{P_i^2}, \qquad S_{\lambda\lambda} \equiv \sum_{i=1}^{n} \frac{N_i M_i^2}{P_i^2}, \tag{11}$$

$$g_\kappa \equiv \sum_{i=1}^{n} \frac{N_i}{P_i}, \qquad g_\lambda \equiv \sum_{i=1}^{n} \frac{N_i M_i}{P_i}, \qquad D \equiv S_{\kappa\kappa} S_{\lambda\lambda} - S_{\kappa\lambda}^2, \tag{12}$$

the least squares solution for the best fit parameters κ and λ of Eq. (1) is [20]

$$\kappa = \frac{\mathrm{g}_\kappa S_{\lambda\lambda} - \mathrm{g}_\lambda S_{\kappa\lambda}}{D}, \qquad \lambda = \frac{\mathrm{g}_\lambda S_{\kappa\kappa} - \mathrm{g}_\kappa S_{\kappa\lambda}}{D} \tag{13}$$

with the covariance matrix

$$\begin{pmatrix} V_{\kappa\kappa} & V_{\kappa\lambda} \\ V_{\lambda\kappa} & V_{\lambda\lambda} \end{pmatrix} = \frac{1}{D} \begin{pmatrix} S_{\lambda\lambda} & -S_{\kappa\lambda} \\ -S_{\kappa\lambda} & S_{\kappa\kappa} \end{pmatrix}, \tag{14}$$

and the error induced to the extracted top-quark mass is

$$(\delta M_{\mathrm{top}})_{\mathrm{fit}} = \frac{\sqrt{V_{\kappa\kappa} + 2M_{\mathrm{top}} V_{\kappa\lambda} + M_{\mathrm{top}}^2 V_{\lambda\lambda}}}{\lambda} = \\ = \frac{1}{\lambda} \sqrt{\frac{S_{\lambda\lambda} - 2M_{\mathrm{top}} S_{\kappa\lambda} + M_{\mathrm{top}}^2 S_{\kappa\kappa}}{D}}. \tag{15}$$

For a (nearly) diagonal covariance matrix, the errors in the fit parameters are $\delta\kappa = \sqrt{V_{\kappa\kappa}} = \sqrt{S_{\lambda\lambda}/D}$ and $\delta\lambda = \sqrt{V_{\lambda\lambda}} = \sqrt{S_{\kappa\kappa}/D}$. Then Eq. (15) goes over to Eq. (5).

Using Eqs. (11), (12), the determinant $D(> 0)$ of the covariance matrix is written as follows:

$$D = \sum_{i=1}^{n} \sum_{j=1}^{n} \frac{N_i N_j M_i^2}{(P_i P_j)^2} - \sum_{i=1}^{n} \sum_{j=1}^{n} \frac{N_i N_j M_i M_j}{(P_i P_j)^2}. \tag{16}$$

We assume that the statistics is the same for all simulations, i. e., that $N_i \equiv N \Rightarrow N_{\mathrm{total}} = N \cdot n$ for all $i = 1, \ldots, n$. Then

$$D = N^2 \sum_{i=1}^{n} \sum_{j=1}^{n} \frac{M_i (M_i - M_j)}{(P_i P_j)^2}. \tag{17}$$

The last form of D transforms to

$$D = N^2 \sum_{i=j}^{n} \sum_{j=1}^{n-1} \left(\frac{M_i - M_j}{P_i P_j} \right)^2. \tag{18}$$

On the other hand, using again Eqs. (11), (12),

$$S_{\lambda\lambda} - 2M_{\rm top}S_{\kappa\lambda} + M_{\rm top}^2 S_{\kappa\kappa} = N\sum_{k=1}^{n}\left[\left(\frac{M_k}{P_k}\right)^2 - \frac{2M_k M_{\rm top}}{P_k^2} + \left(\frac{M_{\rm top}}{P_k}\right)^2\right]. \tag{19}$$

Combining Eqs. (15), (18) and (19) together, we find

$$(\delta M_{\rm top})_{\rm fit} = \frac{1}{\lambda\sqrt{N}} \times \left[\sum_{k=1}^{n}\left(\frac{M_k - M_{\rm top}}{P_k}\right)^2 \Bigg/ \sum_{i=j}^{n}\sum_{j=1}^{n-1}\left(\frac{M_i - M_j}{P_i P_j}\right)^2\right]. \tag{20}$$

Equation (20) shows that the accuracy of the linear fit can be increased in three ways: (i) By raising the statistics at each mass point, i. e., increasing the number N of Monte Carlo events passing all of the selection cuts after simulation. (ii) By increasing the number n of mass points. Then more terms, all of them being positive, are added to both sums in the numerator and in the denominator of the right-hand side, but the number of terms in the simple sum of the numerator is n whereas the number of terms in the double sum of the denominator is $n(n–1)/2$. (iii) By extending the scanned mass range. Then the quadratic differences $(M_i - M_j)^2$ in the denominator at the most distant points [for example, $(M_n - M_1)^2$] increase more rapidly than the quadratic differences $(M_k - M_{\rm top})^2$ in the numerator [for example, $(M_n - M_{\rm top})^2$ or $(M_{\rm top} - M_1)^2$], assuming that the finally extracted $M_{\rm top}$ is located at or near the middle of the range. Among the three possible ways, (i) is more efficient than (ii) and (ii) is more efficient than (iii). But for a global optimization of the fit, all three ways must be tried. For a fixed mass range, the systematic error in the top-quark mass coming from the fit decreases approximately as $1/\sqrt{N\cdot n} = 1/\sqrt{N_{\rm total}}$ with raising global statistics.

Increasing the accuracy of the fit, especially by extending the mass range, will allow for a study of the importance of nonlinear terms which, according to the discussion in Appendix A, are expected to manifest themselves at least near the threshold $M_{\rm top} = M_W + M_b = 85$ GeV/c^2. Exact χ^2 criteria must then be carefully applied in order to exhaust the possibility of further improving the accuracy of the fit by better modelling the relationship between $\langle P_T\rangle$ and $M_{\rm top}$.

Acknowledgements. This work has been partly supported by the Greek General Secretariat for Research and Technology, by the EEC RTN contract HPRN-CT-2002-00292, by the INTAS-CERN grant 32-52-6477, by the Special Account for Research Grants of the National and Kapodistrian University of Athens, and by the EPEAEK II program (Operational Program for Education and Initial Training) in the framework of the projects «Pythagoras» and «Herakleitos».

REFERENCES

1. *Campagnari C., Franklin M.* // Rev. Mod. Phys. 1997. V. 69. P. 137.
2. *Affolder T. et al.* // Phys. Rev. D. 2001. V. 63. P. 032003.
3. *Abbott B. et al.* // Phys. Rev. D. 1998. V. 58. P. 052001.
4. *Abe F. et al.* // Phys. Rev. D. 1999. V. 59. P. 092001.
5. *Acosta D. et al.* // Phys. Rev. Lett. 2004 (submitted); FERMILAB-Pub-04/396-E.
6. *Affolder T. et al.* // Phys. Rev. Lett. 2001. V. 87. P. 102001.
7. *Abe F. et al.* // Phys. Rev. Lett. 1995. V. 75. P. 3997.
8. *Abe F. et al.* // Phys. Rev. D. 1995. V. 52. P. 2605.
9. *Arguin J. F. et al.* Measurement of the Top Quark Mass with *in situ* Determination of the Jet Energy Scale // Phys. Rev. D. 2005 (in press).
10. ATLAS Collab. ATLAS Detector and Physics Performance. Technical Report. CERN/LHCC/99-15. 1999.
11. CMS Collab. CMS Detector and Physics Performance. Technical Report. CERN/LHCC/94-38. 1994.
12. *Marchesini G. et al.* // Comp. Phys. Comm. 1992. V. 67. P. 465.
13. CDF II Collab. The CDF II Detector Design Report. Technical Report. FERMILAB-Pub-96/390-E. 1996.
14. *Sjöstrand T., Bengtsson M.* // Comp. Phys. Com. 1987. V. 46. P. 43.
15. *Meyer A. et al.* The CDF Experiment at the Tevatron — The First Two Years of Run II // Mod. Phys. Lett. A. 2002 (submitted); FERMILAB-Pub-03/162-E.
16. *Acosta D. et al.* // Phys. Rev. Lett. 2004. V. 93. P. 142001.
17. *Collins J. C., Soper D. E., Sterman G.* // Nucl. Phys. B. 1986. V. 263. P. 37.
18. *Nason P., Dawson S., Ellis R. K.* // Nucl. Phys. B. 1986. V. 263. P. 37.
19. Particle Data Group // Phys. Lett. B. 2004. V. 592. P. 1.
20. *Bevington P. R., Robinson D. K.* Data Reduction and Error Analysis for the Physical Sciences. 2nd ed. McGraw-Hill, Inc., 1975. Chs. 6–8.

Received on July 8, 2005.

Редактор *Н. С. Скокова*

Подписано в печать 28.09.2005.
Формат 60 × 90/16. Бумага офсетная. Печать офсетная.
Усл. печ. л. 1,18. Уч.-изд. л. 1,67. Тираж 385 экз. Заказ № 55043.

Издательский отдел Объединенного института ядерных исследований
141980, г. Дубна, Московская обл., ул. Жолио-Кюри, 6.
E-mail: publish@pds.jinr.ru
www.jinr.ru/publish/